Review of Scientific Instruments

RESEARCH ARTICLE | JUNE 16 2023

Single thermal scan digital system for deep level transient spectroscopy

D. Sreeshma ; K. S. R. Koteswara Rao

Rev Sci Instrum 94, 063202 (2023)
https://doi.org/10.1063/5.0147102

CrossMark

View Online

Export Citation

18 July 2023 17:05:16

Single thermal scan digital system for deep level transient spectroscopy

Cite as: Rev. Sci. Instrum. 94, 063202 (2023); doi: 10.1063/5.0147102
Submitted: 19 February 2023 • Accepted: 26 May 2023 •
Published Online: 16 June 2023

View Online

Export Citation
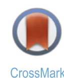
CrossMark

D. Sreeshma,[a] and K. S. R. Koteswara Rao[b]

AFFILIATIONS

Department of Physics, Indian Institute of Science, Bangalore, Karnataka 560012, India

[a]Electronic mail: sreeshma@iisc.ac.in
[b]Author to whom correspondence should be addressed: ksrkrao@iisc.ac.in

ABSTRACT

We have developed a micro-controller based Deep Level Transient Spectroscopy (DLTS) system to identify the deep-level defects in semiconductors. It consists of Arduino-Due, a capacitance meter, and interface circuits. In addition, we have also developed the algorithms needed for the entire signal processing. It is not limited to Arduino-Due but can be implemented using other micro-controllers also. We have used Arduino-Due to generate the filling pulse and monitor the capacitance, temperature, data acquisition, timing control, and signal processing. The sequence of generating the filling pulse, reading the data, and signal processing is controlled digitally rather than by analog sampling circuits and timers. The minimum pulse width generated using Arduino-Due is 50 ns; the pulse width generation depends on various hardware and software parameters and their integration. The resolution in reading the data is 0.8 mV/unit. The time delays in reading the data are appropriately taken care of in the system. The whole experiment can be completed in a single temperature cycle within 2–3 h. The system is simple, inexpensive, in an easy-to-use platform, and less time-consuming; minimizes possible errors; and improves accuracy. The measurements using the "micro-controller based DLTS system" are verified by fabricating (Au) gold-doped silicon (Si) p–n junction samples (Au is a well-understood defect in Si). Using the Arduino-Due based DLTS system, we calculated the energy, the capture cross section, and the concentration of trap levels. The results are in good agreement with the literature, indicating the versatility of the system.

Published under an exclusive license by AIP Publishing. https://doi.org/10.1063/5.0147102

18 July 2023 17:05:16

I. INTRODUCTION

Identifying trap or defect levels in the bandgap of semiconductor materials and the heterostructures' interfaces is of paramount interest because of the detrimental effect of these traps on the semiconductor device's performance.[1–3] Defects perturb the semiconductor lattice, which can raise electronic states in the bandgap, cause degradation, and limit the device's performance.[4] The deep defect states are responsible for leakage due to the thermal generation of carriers via these states.[5] They can also act as recombination centers, which reduce the carrier lifetime and, thus, optimize optoelectronic devices, such as solar cells[6] and light-emitting diodes.[7,8] The trapping and release of carriers from the deep states produce noise and instability in some devices. In some cases, the defects are helpful, especially when the concentration of the defects is large, so the lifetime of the carriers is in picoseconds; we can use them as a material for ultrafast optoelectronic switching or to optically generate THz pulses.[9,10] The deep states can act as luminescence centers in wide bandgap materials to emit light at specified wavelengths.[11] All these require control over these defect levels. Such control, in turn, requires accurate knowledge about the trap levels.

Historically, thermally stimulated current techniques were used to study the deep defects.[12] If the concentration of deep states is comparable to or more than the number of free carriers, then with the increase in temperature, the bulk conductivity will change due to the release of carriers from traps. This thermally stimulated current (TSC) technique is applied to bulk samples rather than junctions and is rarely used nowadays. The thermally stimulated capacitance (TSCAP) technique is equivalent to TSC to look at changes in the capacitance.[12] In this technique, the depletion capacitance is measured as a function of temperature after filling the traps with carriers. It is difficult to measure the trap levels' activation energy in both these methods, although an estimate can be made. Lack of sensitivity, poor discrimination between different defect states, and difficulties in quantifying defect properties are the drawbacks of this method. This was overcome by the invention of Deep Level Transient Spectroscopy (DLTS).

Published under an exclusive license by AIP Publishing

DLTS introduced by Lang is a high−frequency capacitance transient−based thermal scanning method useful to identify a variety of trap levels in semiconductor materials.[13] It gives information about the electrically active defects, and the simplicity of this technique is that the trap appears as a peak in the DLTS spectrum against temperature, so the analysis is straightforward. This can give information about the defect level energy, the concentration of defect levels, and the capture cross section and distinguish between minority carrier and majority carrier traps. The signals due to different traps can be resolved easily, and it is highly sensitive, capable of detecting a small concentration of the defect states. In this method, we make use of the depletion capacitance of a PN junction or Schottky junction. The capacitance of the depletion region will change with time if deep-level defects are present in the material. So, when voltage is applied across the junction, the capacitance changes due to the change in free carriers in the depletion region. If deep levels are present, a capacitance transient is observed over time due to the emission of trapped carriers from the deep states. The standard measurement setup of DLTS is based on a boxcar system that operates in the noise spectrum and combined with the inherent signal averaging.

An elemental DLTS spectrometer consists of a cryostat, a pulse generator, a capacitance meter, a signal processing unit, and digital multimeters.[14,15] The signal processing unit consists of a rate window circuit, a signal analyzer, and a clock synchronizing circuit. The rate window circuit is used to fix the time base for the entire DLTS, sets the rate window timings, and controls the sequence of events in the DLTS experiment. The signal analyzer is used to extract the hidden information in a series of capacitance transients. The clock synchronizing circuit provides the necessary time synchronization between the pulse generator, which provides the filling pulse to the sample, and the signal processing unit, which sets the rate window timings. The DLTS method is based on fixing the emission rate window, and the measurement apparatus responds only when there is a transient with a rate within this window. The emission rate of the trap levels varies with temperature. So if we change the emission rate by varying the temperature, we get a response peak at a temperature where the emission rate falls within the rate window fixed. The measurement procedure starts with selecting the rate window timings, varying the temperature from 77 to 300 K, recording the response peak, and repeating it for other rate windows. The peak position gives information about the emission rate and then the energy level of traps. The main issue with this measurement setup is that when it goes through many temperature cycles, the adhesion of the thin film to the substrate and the device contact may become poor. Keeping the same temperature ambiance at each measurement is difficult. All these things lead to the poor quality of the data.

In this work, "a micro-controller based instrument for deep level transient spectroscopy" is developed to investigate the deep-level defects present in the bandgap of semiconductor materials. The micro-controller based DLTS system includes only the capacitance meter and the Arduino-Due based circuits. We have used Arduino-Due to generate the filling pulse, to read the capacitance meter and temperature, and we have developed algorithms for the entire signal processing that consists of information on the temperature of the sample, capacitance transient, and their storage, and getting the DLTS signal for different rate windows as a function of temperature. The minimum pulse width generated using Arduino-Due is 50 ns, and the resolution in reading the data is 0.8 mV/unit. The time delays in reading the data are appropriately taken care of in the system. The system's performance is tested by carrying out measurements of activation energy, capture cross section, and concentration of trap levels on gold-doped silicon.

II. FABRICATION OF THE DEVICE

We have used neutron transmutation-doped silicon of resistivity 200 Ω cm as a starting material for our experiment. The aluminum (Al) and gallium (Ga) are diffused deeply into the sample for 48 h at a very high temperature of 1200 °C. The junction depths are around 90 μm. After Al and Ga diffusion, phosphorus is selectively diffused. On the backside of the wafer, gold is vacuum evaporated and diffused for 2 h at 800 ± 5 °C in flowing nitrogen. Thus, the prepared samples have $n+-p-n-p-n+$ structures.[16]

For the DLTS experiments, we need a single p–n junction. So, we removed the outer two n+ layers by mechanical lapping. Thus, the formed p–n junction is cleaned in an ultrasonic bath and then dipped in trichloroethylene for cleaning and degreasing, and then, it was cleaned using acetone and methanol. To remove the native oxide, we dipped it in hydrofluoric acid (HF) and then cleaned it with DI water and methanol. Since the background doping of the thyristor samples is low ($\approx 5 \times 10^{13}$ cm^{-3}), large area (around 3×3 mm^2) samples are cut from the wafer.

For ohmic contacts, nickel is deposited on both sides of the junction by electroless plating. For nickel electroless plating, we prepared the nickelex solution by mixing nickel chloride (30 g/l), sodium hypophosphite (10 g/l), ammonium citrate (65 g/l), and ammonium chloride (50 g/l) in DI water and heating it to 80 °C.[17] The sample is dipped into the nickelex solution and heated it to 80 °C. A little amount of ammonia solution is added if the deposition is not happening. The sample was kept in the solution for 15 min after the deposition starts. The nickel will be coated all over the sample. We have to remove the nickel coated at the edges. For that, we cover the upper and lower parts of the sample with wax and then slowly added diluted nitric acid at the edges only. The nickel coated on the edges of the sample is removed, and the edges are polished with the CP4 etchant for 1 h to avoid edge effects. The CP4 etchant solution is prepared by mixing hydrofluoric acid, nitric acid, and acetic acid in the ratio of 1:3:8, respectively. Thus, the prepared samples are used for checking the micro-controller based DLTS system.

III. RESULTS AND DISCUSSION

A. Instrumentation

The complete block diagram of the micro-controller based deep level transient spectroscopy system is shown in Fig. 1. The Arduino-Due based circuit is used to generate the filling pulse, to read the capacitance meter and temperature, and we have developed algorithms for the entire signal processing.

1. Pulse generator

One of the essential parts of the DLTS system is the pulse generator. To extract all the information regarding the deep level defects, we need to apply a pulse of varying width and height. The height and

18 July 2023 17:05:16

Published under an exclusive license by AIP Publishing

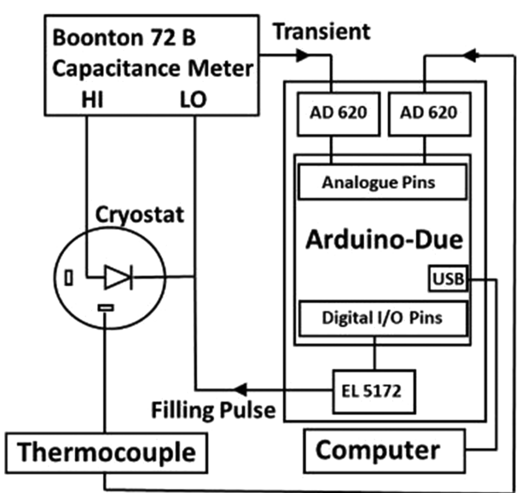

FIG. 1. The complete block diagram of the Arduino-Due based deep level transient spectroscopy system.

width of the pulse depend on the device junction properties. Typically, we need a pulse height from negative to 0 V, and the width varies from nanoseconds to seconds. We have developed a pulse generator based on the Arduino Due for DLTS purposes. Arduino is an open-source electronics platform based on easy-to-use software-controlled hardware. Arduino boards are equipped with a variety of microprocessors or micro-controllers. We can send instructions to the micro-controller on the board, and the board works according to these instructions. To do so, we use the Arduino programming language and Arduino software IDE based on processing. We can write programs using the Arduino Integrated Development Environment (IDE) or Arduino software and upload them to an Arduino board. The Arduino board can read the input and turn it into output based on the instructions we fed to the board. The advantages of using an Arduino board are that it is simple, flexible, and inexpensive. It simplifies the process of working with micro-controllers. It is a cross-platform, and it has a clean programming environment. There are different types of Arduino boards depending on the processors. We need a high-frequency processor-based Arduino board to generate a nanosecond (ns) pulse in our work.

Arduino-Due has an 84 MHz AT91SAM3X8E processor. So, we have chosen Arduino-Due in our work. The Arduino-Due is a micro-controller board based on the Atmel SAM3X8E ARM Cortex–M3 CPU. Arduino-Due is the first Arduino board based on a 32-bit ARM core micro-controller. It has 54 digital input/output pins [of which 12 can be used as Pulse Width Modulation (PWM) outputs], 12 analog inputs, four Universal Asynchronous Receiver/Transmitter (UARTs) (hardware serial ports), an 84 MHz clock, an USB OTG capable connection, and two DAC (digital to analog) pins. In the Arduino-Due, the clock frequency is 84 MHz. We could generate a minimum pulse width of 50 ns. The pulse height can vary from 0 to 3.3 V, and the width can range from 50 ns to seconds. The pulse generated using Arduino-Due is shown in Fig. 3. The kind of pulse we need for DLTS purposes should vary from −3.3 to 0 V so that the device junction will go from deep depletion to depletion. As it is a digital system, using Arduino, we cannot generate negative pulses, so we must convert the pulses produced using Arduino. A high-frequency device compatible with Arduino-Due is chosen to convert such a small pulse. We have cautiously selected EL5172 amplifiers for this purpose. The EL5172 is a wide bandwidth, low power, and single-channel differential to a single-ended amplifier. The EL5172 has a −3 dB bandwidth of 250 MHz when connected with a gain of 1 and driving a 500 Ω load. The output voltage of the EL5172 is equal to the difference in input voltages plus the reference voltage and then times the gain,

$$V_0 = \left(V_{in}^{+} - V_{in}^{-} + V_{REF}\right) \times \left(1 + \frac{R_F}{R_G}\right), \tag{1}$$

where V_{in}^{+} is the non-inverting input, V_{in}^{-} is the inverting input, V_{REF} is the reference input, R_F is the feedback resistor, and R_G is the resistor connected from feedback to ground. For an application that requires a gain of 1, short the output pin to the feedback pin. For our requirement, we fixed the gain at 2, connected the inverting pin to

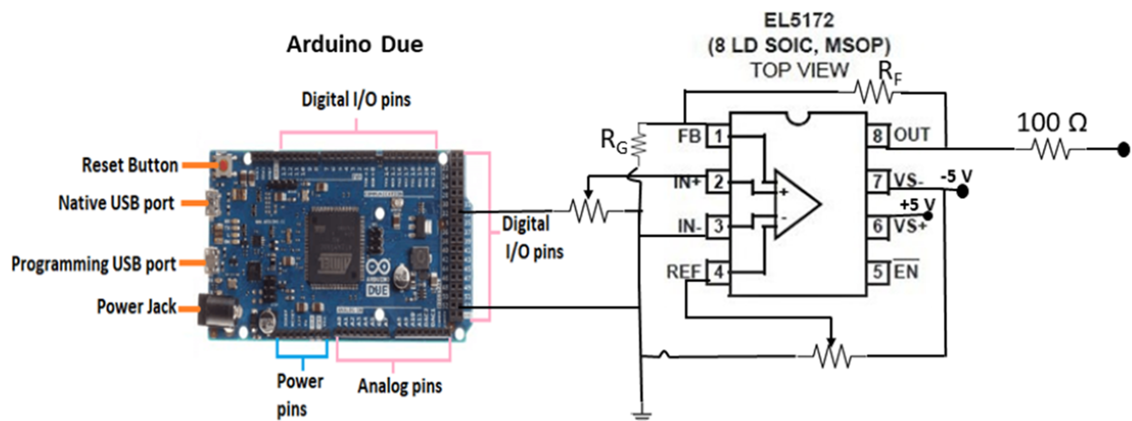

FIG. 2. The circuit diagram of the Arduino–Due based pulse generator.

18 July 2023 17:05:16

Published under an exclusive license by AIP Publishing

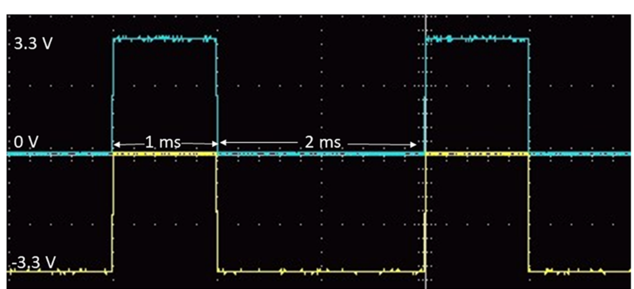

FIG. 3. The 1 ms pulse generated by Arduino-Due (top), output of EL5172 (bottom).

the ground, and applied a negative voltage at the reference pin. So, the output voltage

$$V_0 = (V_{in}^{+} + V_{REF}) \times 2. \tag{2}$$

We have used a series resistor of 100 Ω at the output to eliminate peaking. The power supply pins are bypassed to reduce the risk of oscillation. A single 4.7 μF tantalum capacitor in parallel with a 0.1 μF ceramic capacitor is placed at each supply pin to the ground. The pulse has a rise and fall time of 20 ns each. The complete diagram of the Arduino-based pulse generator and the output generated are given in Figs. 2–4, respectively.

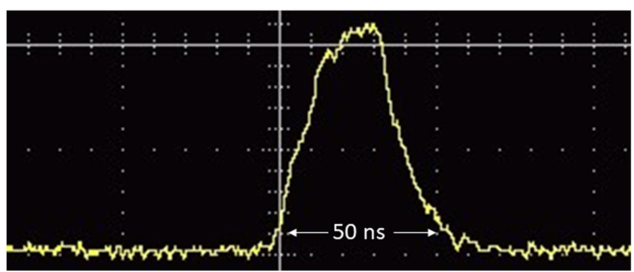

FIG. 4. The 50 ns pulse generated by Arduino−Due (output of EL5172).

B. Reading the data using Arduino–Due

1. Reading capacitance meter output

After applying the pulse to the device, we measure the device's capacitance using a capacitance meter (Boonton 72 B). The output of the capacitance meter is an analog voltage, and we read it using Arduino-Due analog to digital converters. The Arduino-Due board has 12 analog inputs, of which each can provide a 12 bit resolution (i.e., 4096 different values). It measures from ground to a maximum voltage of 3.3 V. So, the Arduino-Due board's resolution is

$$Resolution = \frac{(3.3 - 0)}{4096} = 0.8 \text{ mV/unit}. \tag{3}$$

The analog output of the capacitance meter is given at the non-inverting output of the AD620, and the inverting input is grounded. The capacitance values are read with respect to the ground. To reduce the noise in the measurement, we have added a buffer circuit based on an AD 620 instrumentation amplifier at the output of the capacitance meter and at the input of the Arduino-Due. To further reduce the noise, an RC filter of time constant 1 μs is added at the input of first buffer circuit. The circuit diagram is given in Fig. 5. The transient data read using Arduino-Due are shown in Fig. 6.

2. Reading thermocouple output

We have used Arduino-Due to read the sample's temperature measured using a type T thermocouple. For a type T thermocouple, at room temperature, the voltage varies by 41 μV/°C. It requires a high gain stage before analog to digital conversion. The signal conditioning circuitry typically requires gains of about 500. The difficulty here is distinguishing the actual signal from the noise picked up on the thermocouple leads. To extract the signal from the noise, we have used an instrumentation amplifier AD620 that requires only an external resistor (R_G) to set the gain (G) from 1 to 10 000,

$$R_G = \frac{49.4k\Omega}{G - 1}. \tag{4}$$

Most of the noise appears on both wires; measuring differentially eliminates it. The AD620 works well as a preamplifier due to its low input voltage noise of 9 nV/$\sqrt{Hz}$ at 1 kHz, 0.28 μV p–p in the 0.1–10 Hz band, and 0.1 pA/$\sqrt{Hz}$ input current noise. R_G used

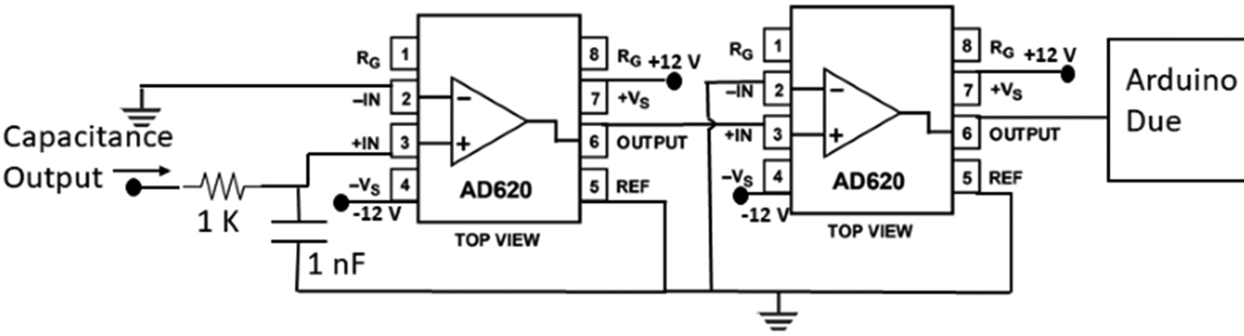

FIG. 5. The circuit diagram to read the capacitance using Arduino−Due.

18 July 2023 17:05:16

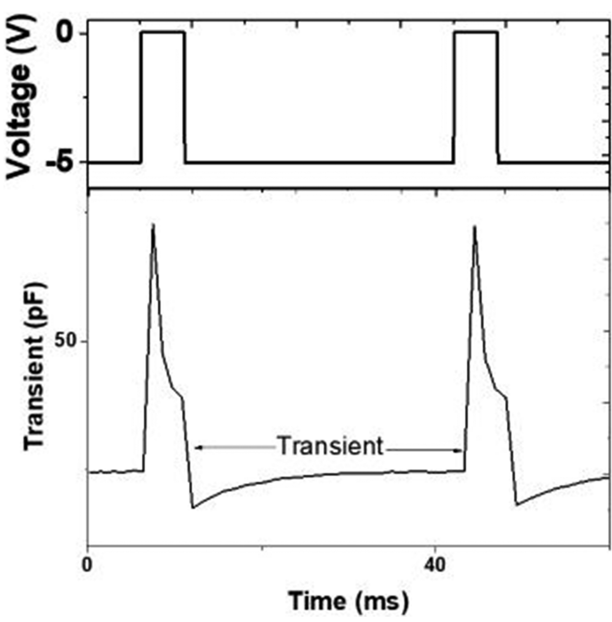

FIG. 6. The transient data (output of the capacitance meter) of an Au-doped Si sample read using Arduino-Due.

in our circuit is 100 Ω. Arduino−Due cannot read negative voltages. At the input of the second AD620, we applied a voltage of 2.4 V, so the output of the AD620 stays positive at all temperature ranges. The complete diagram of the reading temperature of a type T thermocouple using Arduino−Due is given in Fig. 7.

3. Signal processing using Arduino-Due

The Arduino-Due reads the output transient of the capacitance meter every 10 μs and averages over 100 values that gives a data point for every 1 ms. We get the values at each 1 ms, up to the most extended time base value of 3 s (i.e., 3000 points for a change in temperature of 0.05–0.1 K). In addition to hardware signal averaging, this helps us to further reduce the noise in the capacitance transient. Moreover, Arduino-Due records the temperature for every 1 ms up to 3 s and gives out its average. Here, we make sure that the temperature remains constant over this period of time (the change in cryostat temperature is ≈1 K/m). At this stage, we have the temperature and the corresponding transient values at each 1 ms, which is used to extract DLTS data for the required rate windows in a single temperature scan.

The DLTS technique involves finding the time constant of the capacitance transient at different temperatures and finding its maximum by using a boxcar rate window method that can be current, charge, or capacitance transients. Here, we focused on the DLTS based on the capacitance transient. Assume that the capacitance transient $(C-t)$ follows exponential time dependence;[18] then,

$$C(t) = C_0\left[1 - \frac{n_T(0)}{2N_D}\exp\left(-\frac{t}{\tau_e}\right)\right], \tag{5}$$

where C_0 is the capacitance of a device with no deep level impurities involved at reverse bias −V, $n_T(0)$ is the initial steady state trap density, N_D is the concentration of donor ions, and τ_e is the emission time constant. τ_e depends on the temperature as

$$\tau_e = \frac{\exp\left(\frac{E_C - E_T}{k_B T}\right)}{\gamma_n \sigma_n T^2}, \tag{6}$$

where E_C is the conduction band energy, E_T is the trap level energy, σ_n is the capture cross section, with $\gamma_n = \left(\frac{v_{th}}{T^{1/2}}\right)\left(\frac{N_C}{T^{3/2}}\right) = 2\sqrt{3}m_n k_B^2\left(\frac{2\pi}{h^2}\right)^{3/2}$, v_{th} is the thermal velocity of electrons, $v_{th} = \sqrt{\frac{3k_B T}{m_n}}$, N_C is the effective density of state in the conduction band, $N_C = 2\left(\frac{2\pi m_n k_B T}{h^2}\right)^{3/2}$, m_n is the electron density of state effective mass, k_B is the Boltzmann constant, T is the temperature, and h is the Planck constant.

The time constant τ_e decreases with increasing temperature.

The capacitance transient waveform is typically falsified with noise, so the central part of DLTS is to extract the signal from the noise in an automated manner. The technique usually used is a correlation technique. In this signal processing method, multiply the

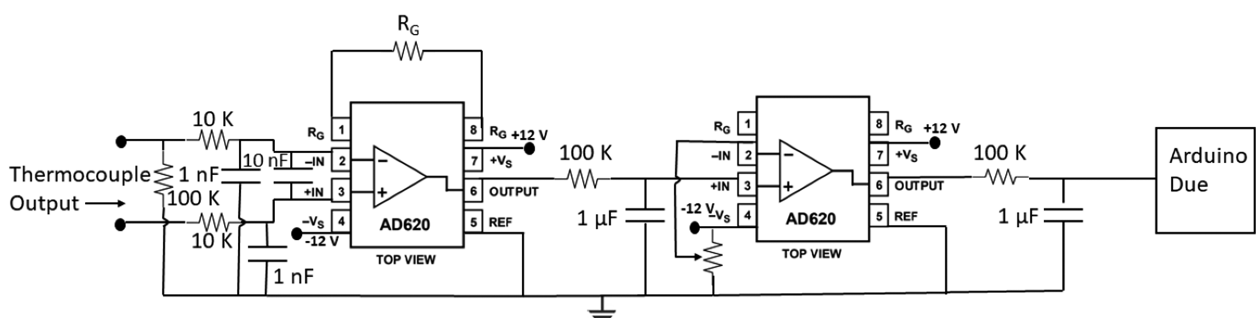

FIG. 7. The circuit diagram to read the temperature using Arduino-Due. The type T thermocouple output is fed to the above circuit to amplify the voltage, avoid noise, and be read by the Arduino-Due.

18 July 2023 17:05:16

Published under an exclusive license by AIP Publishing

input signal by a reference signal called the weighing function $w(t)$. The correlator output is

$$\delta C = \frac{1}{T}\int_0^T f(t)w(t)dt = \frac{C_0}{T}\int_0^T\left(1 - \frac{n_T(0)}{2N_D}\exp\left(\frac{-t}{\tau_e}\right)\right)w(t)dt, \quad (7)$$

where T is the period. The DLTS signal is obtained using the weighing function $w(t) = \delta(t - t_1) - \delta(t - t_2)$ as

$$\delta C = C(t_1) - C(t_2) = \frac{n_T(0)}{2N_D}C_0\left(\exp\left(\frac{-t_2}{\tau_e}\right) - \exp\left(\frac{-t_1}{\tau_e}\right)\right), \quad (8)$$

where $T = t_1 - t_2$. δC exhibits a maximum at a temperature T_1. The value of $\tau_{e,max}$ at $\delta_{C,max}$ is

$$\tau_{e,max} = \frac{t_2 - t_1}{ln\left(\frac{t_2}{t_1}\right)}. \quad (9)$$

Thus, the emission rate corresponding to the maximum of a trap peak observed in a DLTS thermal scan is a precisely defined quantity and may be used along with the temperature corresponding to the peak maximum in constructing a semilog activation energy plot. That is to say, at the maximum of the DLTS signal, one can measure the temperature and calculate $\tau_{e,max}$ to get one point of a $\log\left(\frac{1}{\tau_e}\right)$ vs $\left(\frac{1000}{T}\right)$ Arrhenius plot. We get similar points for other rate windows, and the slope of the resulting linear fit gives the activation energy. In the usual DLTS setup, a dual-gated signal averager (double boxcar) is used to precisely determine the rate window and to do the signal averaging to enhance the signal–noise ratio. The boxcar output monitored using both a multimeter and the Arduino–Due is compared in Fig. 8.

The system we have developed also makes use of the two-point correlation method discussed above. However, we measure and store the capacitance transient data and the temperature using Arduino-Due. After the 5 ms filling pulse, a delay of 10 μs is provided before the Arduino-Due starts reading the data. Then, an average of 100 values at 10 μs intervals is collected to get the data point for every 1 ms, which was repetitively taken for a period of 3000 ms (3 s). Thus, the acquired transient data using Arduino–Due with and without averaging are compared in Fig. 9 (up to a value of 35 ms). The transient measured using a boxcar is given in the supplementary material (Sec. B). The rate of change in temperature of the cryostat is kept at 1 K/m (equivalent to 0.05 K for every 3 s) such that we make sure that the temperature stays almost constant during the repetitive period of 3 s. Approximately for a change in temperature of 0.05 K, we have one complete transient datum and the corresponding temperature. Then, the Arduino-Due sends the next filling pulse and repeats the data collection procedure. In a single temperature scan (77–310 K), we have the complete transient data at different temperatures, which are used to deduce the defect activation energies and related information.

To enhance the signal to noise ratio, we further did the digital filtering to the transient signal. The transient data before and after this digital filtering are compared in Fig. 10.

Now that we have the transient vs temperature data with a better signal to noise ratio, we need to draw out the DLTS spectrum to find the trap level energy. We follow the rate window concept, considering the time base (T_B) at 1, 2, 4, 10, 20, 40, 100, and 200 ms. The difference in capacitance transient data is found where the rate

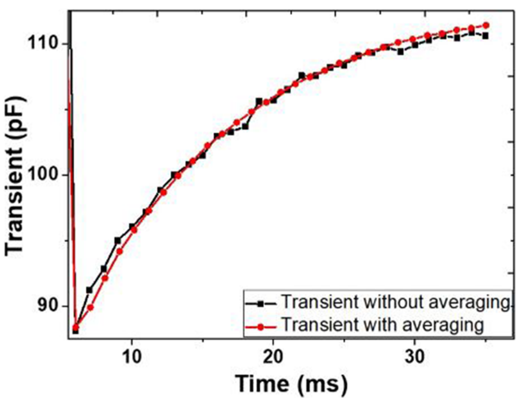

FIG. 9. The transient data of an Au-doped Si sample read at 1 ms gap without averaging and the transient data read at 10 μs gap averaged 100 values to get 1 ms data are compared.

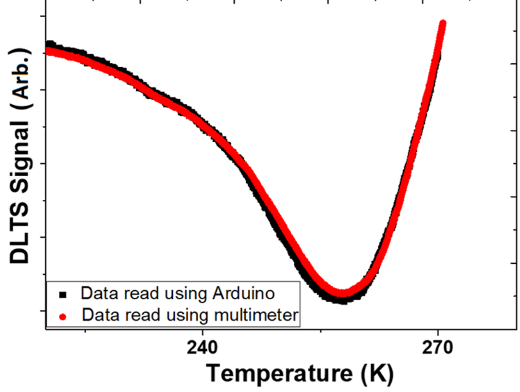

FIG. 8. The output of the boxcar integrator and the temperature measured using a Keithley 2000 multimeter and Arduino-Due are compared. The data are for an Au-doped Si sample.

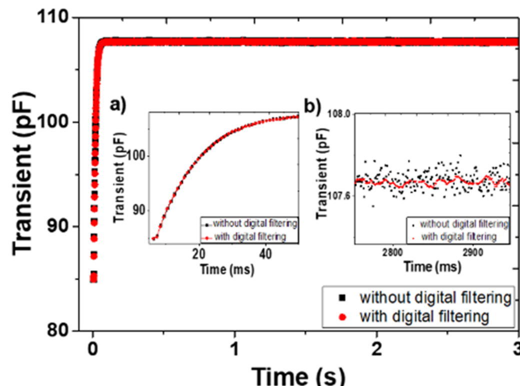

FIG. 10. The transient data of an Au-doped Si sample (averaged 100 times to get 1 ms data) before and after performing digital filtering.

18 July 2023 17:05:16

Published under an exclusive license by AIP Publishing

windows t_1 and t_2 are selected as $3T_B$ and $13T_B$, respectively. Considering the time delays in reading the data, the rate windows are calculated as follows:

$$\tau_e = \frac{t_2 - t_1}{ln\left(\frac{t_2}{t_1}\right)} \cong 7.5T_B. \tag{10}$$

We tried with different rate windows like (3,10), (3,13), (3,15), and (1,10), but (3,13) gave the better results when compared with the well-known gold acceptor and donor levels. The difference in capacitance (DLTS signal) vs temperature at different time bases is obtained at a single temperature scan called the DLTS spectrum.

C. Verification of the system

To verify the results of our measurements using an Arduino-Due based DLTS setup, we have fabricated gold-doped silicon (Si) p–n junction samples, which is a well-understood defect in Si. The sample preparation is provided in Sec. II.

The I–V, C–V, C–F, and $1/C^3$ vs V data are given in the supplementary material (Sec. A). From the C–V measurements, it is observed that the device depletion capacitance varies from 160 to 60 pF when the voltage ranges from 0 to −10 V. For DLTS measurements, we applied a reverse voltage of −5 V and the filling pulse varied from −5 V to 50 mV. The pulse width is 5 ms, and the time to the next filling pulse is 3 s. All the data listed in this work are for the gold-doped silicon p–n junction. The DLTS spectrum obtained in a single temperature scan using the Arduino-Due based integrated system at different time bases is shown in Fig. 11. The trap energy levels T_1 (donor) and T_2 (acceptor) are calculated from the Arrhenius plot shown in Fig. 12; thus, the obtained energy values are 0.36 ± 0.02 and 0.53 ± 0.02 eV for T_1 and T_2, respectively. This is in good agreement with the established literature values observed in Au-doped Si.[16,19] The DLTS spectrum obtained while cooling is given in the supplementary material (Sec. B).

The capture cross section of the trap levels can be calculated in two ways. The first plot of $ln(\tau_e T^2)$ vs $\frac{1}{T}$ has a slope of $\frac{E_c - E_T}{k}$ and an intercept on the $ln(\tau_e T^2)$ axis of $ln(\sigma_n \gamma_n)$. $\gamma_n = \left(\frac{v_{th}}{T^{1/2}}\right)\left(\frac{N_C}{T^{3/2}}\right)$, where h is the Planck constant, k is the Boltzmann constant, T is

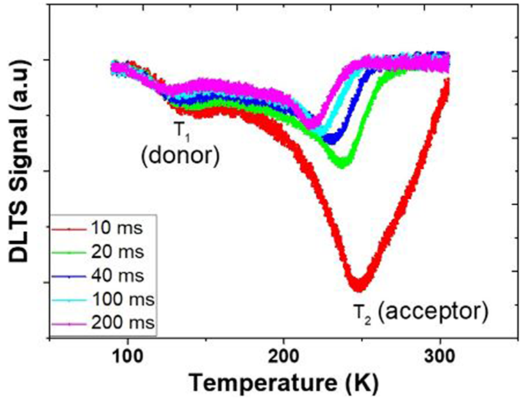

FIG. 11. The DLTS spectrum of Au-doped Si at different time bases. The two trap peaks are marked as T_1 (donor) and T_2 (acceptor).

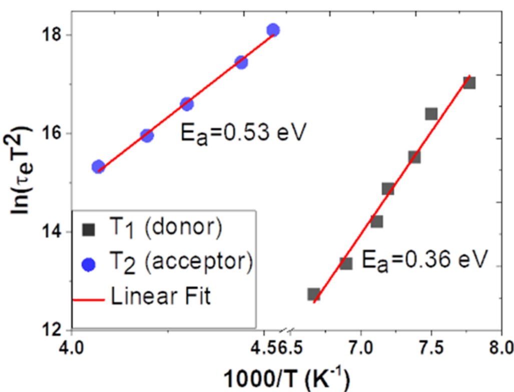

FIG. 12. Arrhenius plot of trap levels T_1 (donor) and T_2 (acceptor) of Au-doped Si. The activation energies are 0.36 and 0.53 eV for T_1 and T_2, respectively.

temperature, and m^* is the effective mass of carriers. The capture cross section calculated from the intercepts are 2.42×10^{-15} and 1.37×10^{-16} cm^2 for traps 1 and 2, respectively.

The capture cross section is also obtained using the variable pulse-width technique. At zero bias, the space charge region gets equilibrated with the neutral region of the device. During this period, the traps get filled with the available charge carriers in the neutral region. The quantum of traps filled depends on the capture probability (capture cross section) and nature of the traps present in the system. If the available time is too short, then only a fraction of traps get filled by charge carriers before it returns to reverse bias. So, when the pulse width varied, the number of traps that gets occupied also changes. We get a saturation value (t_{lp}) when the filling pulse width (t_{lp}) matches the capture time constant (τ_c). The relation between the peak height and the capture pulse width t_p is

$$\frac{1 - \Delta C_{max}(t_p)}{1 - \Delta C_{max}(t_{lp})} = \exp\left(\frac{-t_p}{\tau_c}\right), \tag{11}$$

where $\Delta C_{max}(t_p)$ and $\Delta C_{max}(t_{lp})$ are the maximum values of DLTS signal at t_p (pulse width) and t_{lp} (saturation pulse width), respectively. Thus, the plot of $ln\left(\frac{1-\Delta C_{max}(t_p)}{1-\Delta C_{max}(t_{lp})}\right)$ vs pulse width t_p gives a straight line, and the slope gives $\frac{1}{\tau_c}$. The capture cross sections σ_p, σ_n can be estimated from the relation

$$\sigma_n = \frac{1}{\tau_c v_{th} n}, \tag{12}$$

where τ_c is the capture time constant, v_{th} is the thermal velocity, and n is the density of electrons in the conduction band. This method gives more accurate results. Using Arduino–Due based DLTS system to calculate the capture cross section of the trap levels, we fix the time base at 10 ms and vary the pulse width from 50 ns to 1 ms. First, we set the pulse width at 50 ns to measure the transient corresponding to 50 ns, then change the pulse width to 100 ns to measure the transient, and so on. We ensure that the temperature stays almost constant until the transient data corresponding to all the

18 July 2023 17:05:16

Published under an exclusive license by AIP Publishing

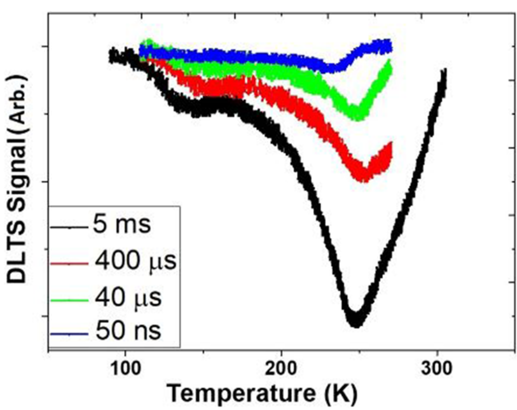

FIG. 13. The DLTS spectrum at different pulse widths for Au-doped Si to find the capture cross section.

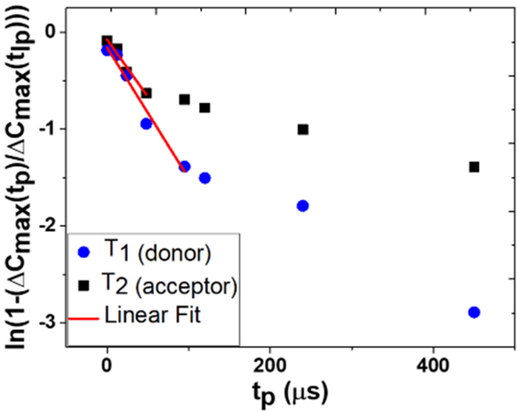

FIG. 14. The $ln(1 - \frac{\Delta C_{max}(t_p)}{\Delta C_{max}(t_{lp})})$ vs t_p graph for trap levels T_1 (donor) and T_2 (acceptor) of Au-doped Si. From the slope, we can calculate the capture cross section of trap levels.

pulse widths are done. So in one temperature run itself, we get all the data corresponding to all the pulse widths. The DLTS spectrum at different t_p is shown in Fig. 13, and the $ln\left(\frac{1-\Delta C_{max}(t_p)}{1-\Delta C_{max}(t_{lp})}\right)$ vs pulse width t_p graph is shown in Fig. 14. The capture cross section values calculated are 5.87×10^{-16} and 1.6×10^{-16} cm^2 for T_1 and T_2, respectively. This is in good agreement with the literature values.[16,19,20]

The concentration of the trap levels is calculated using the method mentioned in the literature for a linearly graded junction. The calculated values are 19.4×10^{11} and $79.1 \times 10^{11}/\text{cm}^3$ for T_1 and T_2, respectively. As in the literature, the concentration of T_2 is four times larger than that of T_1. The value we obtained also was in good agreement with the literature.[16,21]

IV. CONCLUSION

We have developed an Arduino-Due based deep level transient spectroscopy system to identify the deep level defects. The system is simple, inexpensive, in an easy to use platform, and less time-consuming. That we can complete the whole experiment in a single temperature cycle is an added advantage. We have replaced the pulse generator; multimeters used to read the capacitance and the temperature; the sample and hold circuitry; and the dual box car integrator used for the signal processing. The Arduino-Due based DLTS system includes only the capacitance meter and the Arduino-Due based circuits. We focused on completely automating the conventional DLTS and used Arduino-Due to generate the filling pulse, to read the capacitance meter and temperature, and we have developed algorithms for the entire signal processing. The minimum pulse width generated using Arduino-Due is 50 ns, and the resolution in reading the data is 0.8 mV/unit. The time delays in reading the data are appropriately taken care of in the system. We fabricated a gold-doped silicon p–n junction device to test the new system. Using the Arduino-Due based DLTS system, we calculated the energy, the capture cross section, and the concentration of trap levels. We have identified two trap levels with energies Ev+0.36 eV and Ec −0.53 eV; capture cross sections 5.87×10^{-16} and 1.6×10^{-16} cm^2; and concentrations 19.4×10^{11} and $79.1 \times 10^{11}/\text{cm}^3$ for traps 1 and 2, respectively. The results are in good agreement with the literature.

SUPPLEMENTARY MATERIAL

The room temperature I–V, C–V, C–F, $1/C^3$ vs V , the transient graphs, and the DLTS spectrum obtained while cooling the gold-doped silicon p–n junction sample are given in the supplementary material.

18 July 2023 17:05:16

ACKNOWLEDGMENTS

The authors thank Savyan K, M.Tech., IISc Bangalore, for his valuable suggestions.

AUTHOR DECLARATIONS

Conflict of Interest

Intellectual Property. K.S.R.K.R. and D.S. have patent IP-5296-IN-22230269-PA-2022 pending (Indian). The authors have an equal contribution.

Author Contributions

D. Sreeshma: Conceptualization (equal); Data curation (equal); Formal analysis (equal); Investigation (equal); Methodology (equal); Software (equal); Validation (equal); Visualization (equal); Writing – original draft (equal). **K. S. R. Koteswara Rao**: Conceptualization (equal); Project administration (equal); Supervision (equal).

DATA AVAILABILITY

The data that supports the findings of this study are available within the article and its supplementary material.

Published under an exclusive license by AIP Publishing

REFERENCES

[1]D. Bozyigit, S. Volk, O. Yarema, and V. Wood, "Quantification of deep traps in nanocrystal solids, their electronic properties, and their influence on device behavior," Nano Lett. **13**, 5284–5288 (2013).

[2]C. Giansante and I. Infante, "Surface traps in colloidal quantum dots: A combined experimental and theoretical perspective," J. Phys. Chem. Lett. **8**, 5209–5215 (2017).

[3]A. J. Houtepen, Z. Hens, J. S. Owen, and I. Infante, "On the origin of surface traps in colloidal II–VI semiconductor nanocrystals," Chem. Mater. **29**, 752–761 (2017).

[4]H. J. Queisser and E. E. Haller, "Defects in semiconductors: Some fatal, some vital," Science **281**, 945–950 (1998).

[5]A. R. Peaker, V. P. Markevich, and J. Coutinho, "Tutorial: Junction spectroscopy techniques and deep-level defects in semiconductors," J. Appl. Phys. **123**, 161559 (2018).

[6]Z. Jin, A. Wang, Q. Zhou, Y. Wang, and J. Wang, "Detecting trap states in planar PbS colloidal quantum dot solar cells," Sci. Rep. **6**, 37106 (2016).

[7]X. Li, Y.-B. Zhao, F. Fan, L. Levina, M. Liu, R. Quintero-Bermudez, X. Gong, L. N. Quan, J. Fan, Z. Yang *et al.*, "Bright colloidal quantum dot light-emitting diodes enabled by efficient chlorination," Nat. Photonics **12**, 159–164 (2018).

[8]C. Xiang, L. Wu, Z. Lu, M. Li, Y. Wen, Y. Yang, W. Liu, T. Zhang, W. Cao, S.-W. Tsang *et al.*, "High efficiency and stability of ink-jet printed quantum dot light emitting diodes," Nat. Commun. **11**, 1646–1649 (2020).

[9]M. Mittendorff, S. Winnerl, J. Kamann, J. Eroms, D. Weiss, H. Schneider, and M. Helm, "Ultrafast graphene-based broadband THz detector," Appl. Phys. Lett. **103**, 021113 (2013).

[10]E. Lhuillier, M. Scarafagio, P. Hease, B. Nadal, H. Aubin, X. Z. Xu, N. Lequeux, G. Patriarche, S. Ithurria, and B. Dubertret, "Infrared photodetection based on colloidal quantum-dot films with high mobility and optical absorption up to THz," Nano Lett. **16**, 1282–1286 (2016).

[11]A. Alkauskas, M. D. McCluskey, and C. G. Van de Walle, "Tutorial: Defects in semiconductors—combining experiment and theory," J. Appl. Phys. **119**, 181101 (2016).

[12]A. Baldini and M. Bruzzi, "Thermally stimulated current spectroscopy: Experimental techniques for the investigation of silicon detectors," Rev. Sci. Instrum. **64**, 932–936 (1993).

[13]D. V. Lang, "Deep-level transient spectroscopy: A new method to characterize traps in semiconductors," J. Appl. Phys. **45**, 3023–3032 (1974).

[14]L. Jansson, V. Kumar, L.-A. Ledebo, and K. Nideborn, "A sensitive and inexpensive signal analyser for deep level studies," J. Phys. E: Sci. Instrum. **14**, 464 (1981).

[15]C. V. Reddy, S. Fung, and C. D. Beling, "A simple and inexpensive circuit for emission and capture deep level transient spectroscopy," Rev. Sci. Instrum. **67**, 257–261 (1996).

[16]K. S. R. Koteswara Rao, V. Kumar, S. K. Premachandran, and K. P. Raghunath, "Relationship of the gold related donor and acceptor levels in silicon," J. Appl. Phys. **69**, 2714–2716 (1991).

[17]M. V. Sullivan and J. H. Eigler, "Electroless nickel plating for making ohmic contacts to silicon," J. Electrochem. Soc. **104**, 226 (1957).

[18]D. K. Schroder, *Semiconductor Material and Device Characterization* (John Wiley and Sons, 2015).

[19]D. V. Lang, H. G. Grimmeiss, E. Meijer, and M. Jaros, "Complex nature of gold-related deep levels in silicon," Phys. Rev. B **22**, 3917 (1980).

[20]S. D. Brotherton and J. Bicknell, "The electron capture cross section and energy level of the gold acceptor center in silicon," J. Appl. Phys. **49**, 667–671 (1978).

[21]K. S. R. Koteswara Rao and V. Kumar, "Estimation of trap concentration in linearly graded junctions using DLTS," Phys. Status Solidi A **117**, 251–257 (1990).

18 July 2023 17:05:16

Published under an exclusive license by AIP Publishing